Draft version December 16, 2024
Typeset using LaTeX **preprint** style in AASTeX631

A Detailed Observation of the Open Cluster M52

S. Chappelle, A. Chatterji, J. Chowdhury [1]

[1] *Department of Physics and Astronomy, Amherst College, Amherst MA 01002, USA*

ABSTRACT

We present an experimentally developed color-magnitude diagram of the open cluster, Messier Object 52 (M52), whose stars mostly reside on the Main Sequence branch of stellar evolution. Theoretical age and distance were derived from visual, red, and blue band measurements of brightness, obtained from cluster images from the observing night of October 26, 2024. Literature-based isochrones were used to derive the age of the cluster, resulting in an approximated age of 1e8 years, a number which correlates with the commonly accepted values. The distance was then derived by means of the application of the distance modulus equation onto the necessary V magnitude shift of the isochrone to fit the color-magnitude diagram.

1. INTRODUCTION

1.1. *Hertzsprung-Russell Diagram*

A Hertzsprung-Russell (H-R) diagram is a scatter plot (where each point represents a different star) that shows the relationship between the luminosity (or absolute magnitude) and the temperature (or spectral type) of a star. The shape of the distribution conveys valuable information about a given population of stars, mapping out the main sequence and, depending on the age of the stars in the population, further stages in stellar evolution such as the red giant branch and white dwarves. A star is considered to be a blackbody in astronomy, meaning it is a perfect emitter , and the curve representing a blackbody gives insight into both the star's stellar type and temperature. Each blackbody curve for a given temperature has a peak wavelength, corresponding the the star's maximum emission. Short-lived O type stars, for instance, are hotter, bluer, extremely massive, and highly luminous, and they have peak emission in the ultraviolet regime (UV). On the opposite end of the stellar types, the longer-lived M type star is redder and not very massive, this type of star is likely to have its peak emission in the near-Infrared (NIR) regime. This relation is governed by Wien's Law:

$$\lambda_{peak} T = 0.0029\ m \cdot K \tag{1}$$

which can be used to determine the temperature of a star (plotted on the x-axis of an HR Diagram) if given the peak wavelength of emission. On the y-axis, the luminosity of a star, or intrinsic brightness, is determined through measuring the flux, or apparent brightness, and using the known distance to the star in the following relation:

$$f = \frac{L}{4\pi d^2} \tag{2}$$

1.2. *Color-Magnitude Diagram*

Similar to an H-R diagram, a color-magnitude diagram conveys the relationship between color and brightness (magnitude) in a stellar population. The color axis, ranging from blue to red, is to the color-magnitude diagram what the temperature axis is to the H-R diagram. These two axes relate to one another, as bluer stars have hotter temperatures, and likewise redder stars have cooler temperatures. A color is typically calculated by subtracting the magnitude in one band from the magnitude in another, for instance, the commonly used B-V, where B is the B (blue) band magnitude and V is the V (visual) band magnitude. Similarly, the R (red) band magnitude can be used to get the color index V-R.

To complement these choices of color index, the magnitude on the y-axis is usually the V band absolute magnitude, which is the intrinsic brightness in the visual band. Using the measured flux of the star, the apparent magnitude can be calculated as:

$$m_2 - m_1 = -2.5 log_{10}\left(\frac{F_2}{F_1}\right) \tag{3}$$

A standard, zeropoint star, with known flux and magnitude, is required for this calculation. Oftentimes in astronomy, the chosen star is Vega due to its near 0 magnitude across the wavelength spectrum.

Once the apparent magnitude is determined, the absolute magnitude can be determined using the distance modulus and a known distance (d) to the star:

$$m - M = 5log_{10}(d) - 5 \quad (4)$$

1.3. *Clusters*

Star clusters are good candidates for studying stellar populations, as they typically encompass a wide variation of stellar types all around the same relative distance from Earth (the point of observation). Through examining the H-R diagram of a cluster, we can deduce the age of the cluster based on the location of the "turning point", where stars are turning off of the main sequence and onto the red giant branch. The cluster's age will then correspond to the main sequence lifetime of stars in the spectral type at the turning point.

There are two types of star clusters: open and globular clusters. Open clusters are typically younger and contain less stars, whereas globular clusters contain numerous stars that make up an older stellar population. An open cluster's color-magnitude diagram will likely match that of a younger stellar population than for globular clusters, displaying stars along the main sequence and having an earlier turn off point. Open clusters are typically expected to have lifetimes falling between 10 million to a few hundred million years, so we would expect stars of spectral types O and B to be turning off of the main sequence, possibly even A stars if the cluster is on the high end of the age scale. Thus, the color-magnitude diagram of an open cluster will be expected to contain more bluer stars than that of a globular cluster, which will have a turn off point further towards the redder end of the diagram since most of its bluer stars will have evolved off of the main sequence. In this research paper, analyses are performed on an open cluster.

1.4. *Isochrones*

Plotted as a curve on an H-R diagram or color-magnitude diagram, an isochrone is a prediction for a population of stars of varied masses at a specified point in time; this curve prediction assumes the stars are all the same age. These isochrones are formed through simulating the evolution of a varied population of stars for a chosen amount of cosmic time, and then plotting either the temperature and luminosity or color and magnitude (corresponding to the end point in time) onto the diagram.

A pre-simulated isochrone can be compared with a color-magnitude diagram of an open cluster, in which case the best matched isochrone will be considered a good approximation for the age of the cluster.

2. PROCEDURE

2.1. *Telescope Information*

Observations of the cluster M52 are taken using the Amherst College telescope, located on the rooftop of the Science Center. The telescope uses an equatorial mount (Paramount). In addition to this mount, the telescope also has a Moonlite focuser and SBIG CCD (charge coupled device) attached to it. A dew shield was used as a precaution to avoid the formation of dew on the telescope's lens.

With an aperture (lens diameter) of 11 inches, this telescope has an FOV of around 39.856 arcminutes. The telescope has a magnitude limit of 14-15, so stars that are fainter than this will not be detected. Furthermore, the telescope has a pixel scale of 0.64"/pixel and a typical FWHM of 6 pixels, which represents the size of target stars as they appear on camera.

2.2. *Observations*

We provide a table of relevant information regarding the target and standard star observed for this research, as well as information about the choices, settings, and procedure on observing night in Table 1.

2.3. *Conditions on Observing Night*

The observing night was chosen with the most optimal conditions in mind. Firstly, the observing time corresponded to when the cluster of interest would transit highest in the sky, having an airmass of 1.09 as obtained through an online airmass calculator. The standard star transited even higher, having an airmass of 1.00. The moon, having approximate airmass of 1.19, resulted in very little interferance with the observations of the cluster or standard star. Moreover, the weather conditions were clear, with little to no wind or clouds and a medium humidity level. With all of these conditions in mind, it is reasonable to state that we had good seeing for our observations. Using the full-width half max method (FWHM), the seeing was approximated by measuring the FWHM of several small objects in the stacked images. These results were then converted from pixel measurements into arcsecond measurements and averages to obtain a estimated seeing of 4.2 arcseconds. This value aligns with expectations due to higher levels of light pollution from the location choice.

2.4. *Data Reduction Process*

When taking data, it is important to take the necessary calibration frames as well so that the analysis done with the images will be accurate: these calibration frames are bias, dark, and flat frames. Bias frames are taken with 0 second exposures and describe the read

Object Name	Object Type	Right Ascension	Declination	Wavelength (λ)	Exposure Time (s)	Number of Exposures	Total Integration Time (s)	Focus
m52	Open Cluster	23h 24m 46.89s	$+61\circ\ 35'\ 24''$	B	10	10	100	3500
				V	10	10	100	7000
				R	10	10	100	10000
SA 20-245	Standard Star	00h 44m 21.182s	$+45\circ\ 55'\ 12.77''$	B	5	10	50	5000
				V	5	10	50	7000
				R	5	10	50	12000

Table 1. Information regarding the target open cluster M52 and standard star SA 20-245 from Landolt (2013) and the settings and procedure on observing night.

noise for the telescope, which is a product of the detector itself. Dark frames are taken with varying exposures and are taken with the lens cover on (an additional covering can be added like a sheet of fabric to ensure no photons reach the detector). These dark frames are used to account for the noise produced by thermal emission from the telescope, which is why it is better to have the telescope cooled to a certain temperature before beginning to observe. Lastly, flat frames can be taken in multiple different ways, but in the context of this paper the flat frames were twilight flats, achieved by pointing the telescope at a blank patch of the sky at twilight. These frames are crucial in accounting for noise from dust, bugs, or other factors. For this paper, the bias and dark frames were taken the night of observing, and the flat frames were taken on a different night by a separate observing group. We make the assumption that the conditions of the two observing nights are relatively equivalent.

The initial step in the data reduction process is to use these data calibration frames to subtract the sources of noise from the science images. Our Python data reduction pipeline subtracts the median bias, dark, and flat frame images from the science images using the following equations. We first create a master bias file using the multiple 0 second exposure bias frames, taking a 3D median since the median is less succeptible to outliers than the mean.

$$B_M = med_{3D}[B_i] \tag{5}$$

We then create the master dark frame using the same technique, with the added task of subtracting the master bias from each individual dark frame and normalizing by the exposure time before taking the 3D median.

$$D_M = med_{3D}\left[\frac{(-D_i - B_M}{t}\right] \tag{6}$$

Here t is the exposure time per dark frame. Next, we determine the raw master flat frame as the 3D median of the bias and dark subtracted flats, again normalizing by exposure time. The raw master flat must then be normalized again by the median of the raw master flat to obtain the master flat.

$$F_{raw} = med_{3D}\left[\frac{(F_i - B_M}{t} - D_M\right] \tag{7}$$

$$F_M = \frac{F_{raw}}{med[F_{raw}]} \tag{8}$$

Here t is the exposure time per flat frame. These calibrations are then applied to the science images through the following expression, where t is the exposure time of the science image.

$$S_M = \frac{S_{raw} - B_M - tD_M}{F_M} \tag{9}$$

If each image is thought of as a two dimensional array, the effects of the calibration frames on the science images can be considered. For an example of this, we now consider images of the open cluster M52 taken in the V band. We can see in Figure 1, the top left subplot shows the raw science image, and the remaining subplots show the science image after following the calibration steps outlined above, effectively reducing the image to account for sources of noise defined by the bias, dark, and flat frames. Bias subtraction reduces the pixel values significantly over the full span of the image, decreasing the average value by approximately 900. Dark subtraction then works to remove any thermal interferences, which did not have a large effect on the values in this sample image in Figure 1, likely because our telescope was operating in temperatures in the range of 30-35°F. The flat frames are then subtracted from the images and the values are normalized to approximately one.

With these reduced science images, we then utilize the centroiding method of aligning images, as in Figure 2, as well as the shift and stack technique to obtain one stacked image for each filter band. This stacking technique involves taking the 3D median, as it will be less affected by outliers than the mean in the event of dead pixels, cosmic rays, or other interferences. An example

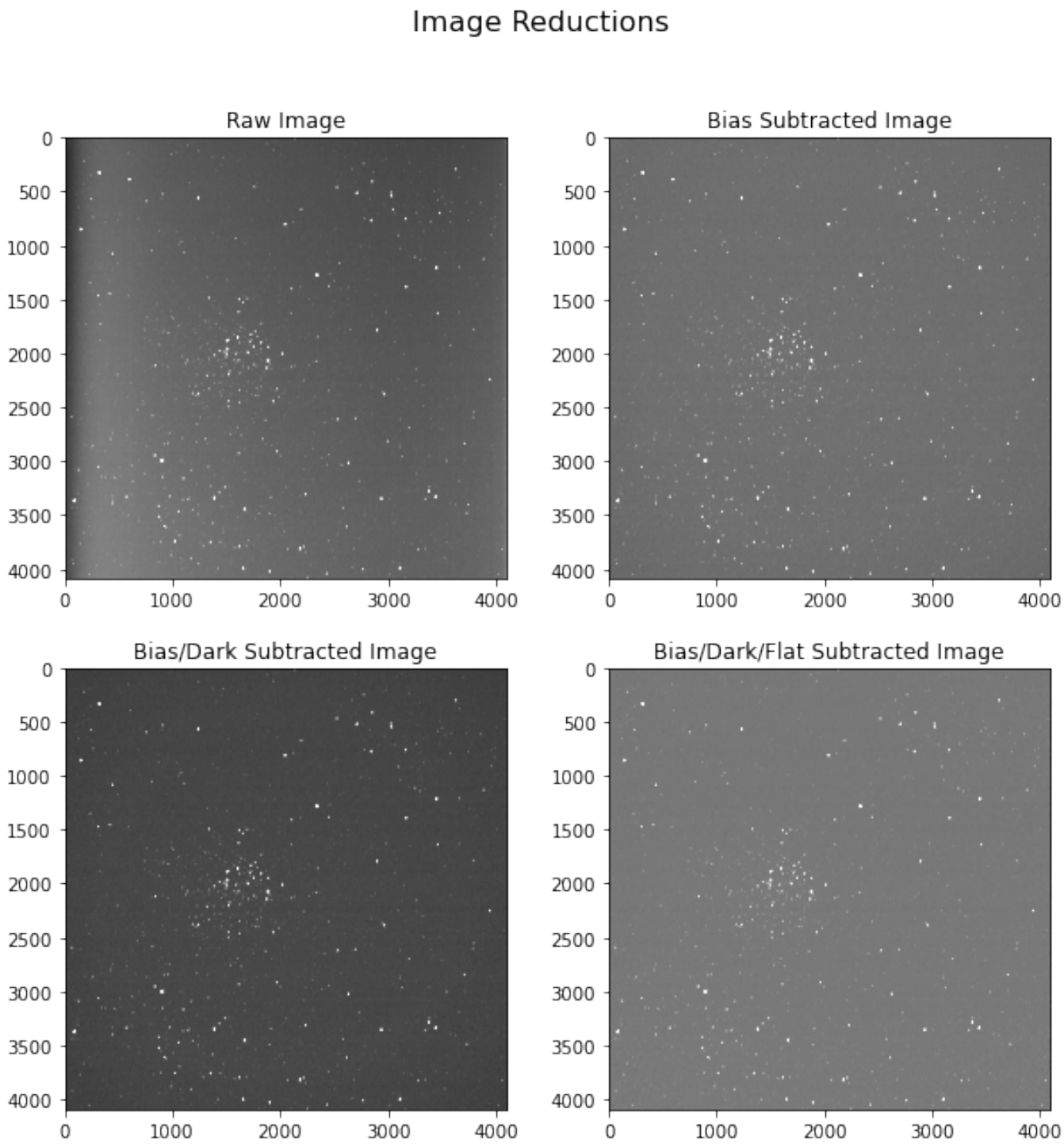

Figure 1. An example of a raw, bias-subtracted, bias/dark-subtracted, and bias/dark/flat-subtracted V-band science image of the cluster M52.

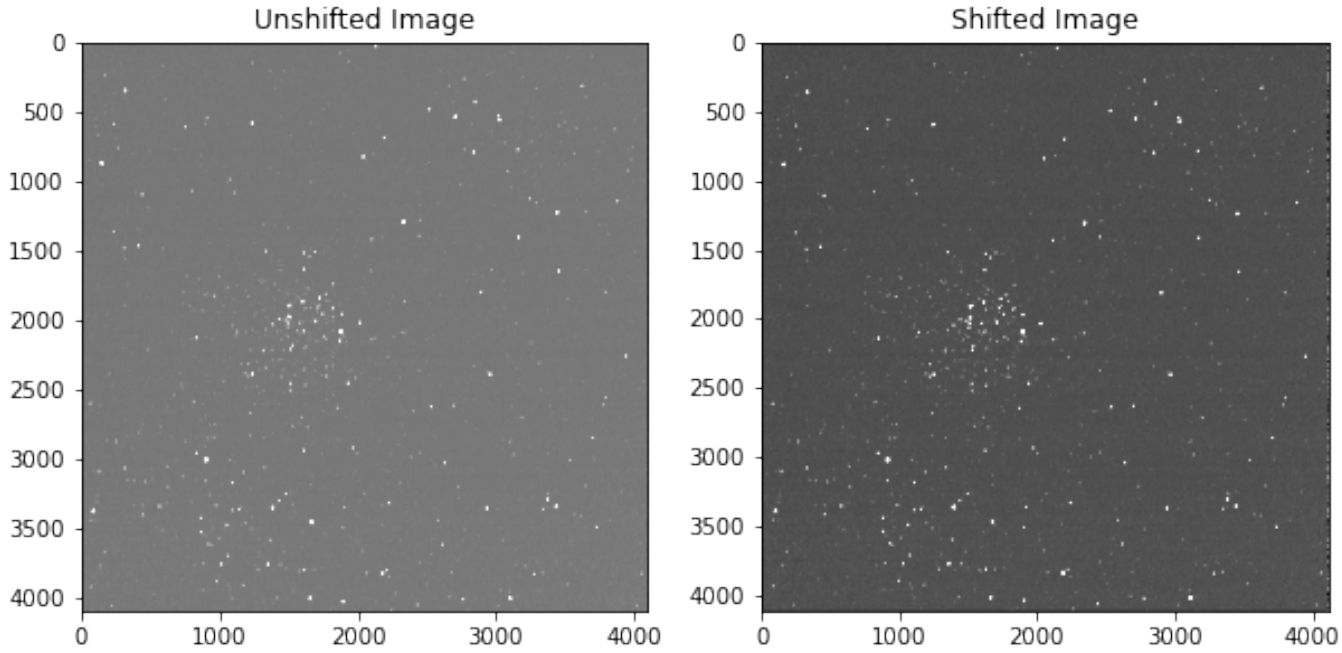

Figure 2. An example of an unshifted and shifted V-band image (note that shifting is relative to the defined reference image, which was always chosen to be the first image in the list for a given filter band.

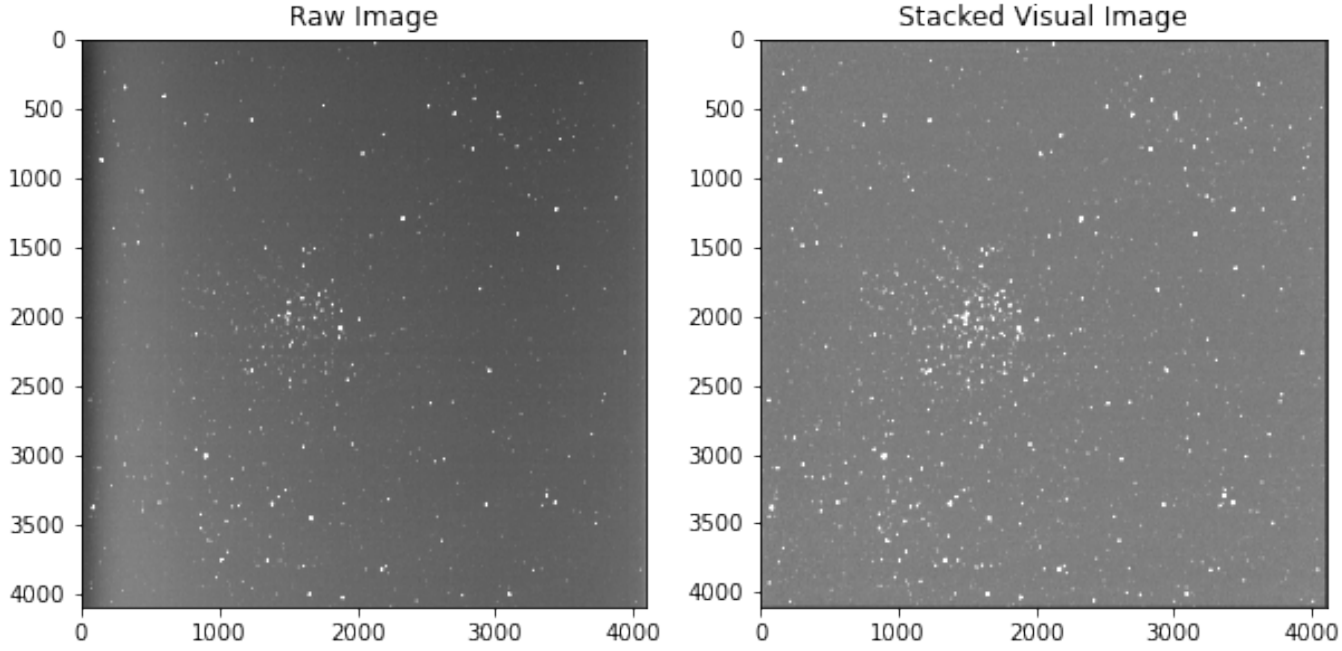

Figure 3. An example of a raw V-band science image and the final stacked image.

Target	Filter	n-σ	FWHM	Number of stars found
M52	V	15	10	586
	B	15	10	553
	R	15	10	596
SA 20-245	V	5	15	264
	B	5	15	240
	R	5	15	352

Table 2. Number of stars extracted for a given value of nsigma for both the cluster and the standard star.

of a raw science image and the total stacked image can be seen in Figure 3.

2.5. *Photometry*

The chosen standard star SA 20-245 can be seen in Figure 4.

In order to ultimately create a color-magnitude diagram, a photometry table detailing information on the stars in the cluster images and the stars in the standard star image was generated. Extracting the data for these stars first requires determining where the stars are located in the image. After choosing a signal to noise ratio threshold for how much brighter the star should be than the background (nsigma), around 500 stars were selected. The mean value of the full width half maximum for the stars was then determined through taking projections of randomly selected stars in an image. DAOStarFinder in Python extracted the stars in the image that satisfied the criteria. A table detailing the number of stars found for tested values of nsigma is shown in Table 2.

The extracted stars are then saved as a region file to be over-plotted onto the images of the cluster and standard star, as seen in Figures 5 and 6, respectively.

2.6. *Aperture Photometry*

Photometry in astronomy refers to measuring the flux of an object of interest. In order to do so, an astronomer needs to define an aperture, or area, within which the star is located. The goal for such an aperture is to ensure that the majority of the star's light is captured, while avoiding having too much empty space (background), both of which could decrease the signal to noise ratio. Thus, it is ideal to have neither too small nor too large of an aperture.

The flux measured within the bounds of the aperture will consist of light from the star (source) as well as other light sources within the circle (background or interference from another star). Note that it is ideal to make sure that there are no other stars within the aperture.

The true flux of the star, which is needed to compute the absolute magnitude, must be background subtracted in order to get rid of the other interfering sources of light; this requires an estimate for the background. Typically, an anulus (ring of inner and outer radius both greater than the radius of the aperture) is chosen such that it contains no other stars and measures the background relatively close to where the star of interest is located. Once the background is estimated within the anulus, it can be subtracted from the flux calculated within the aperture in order to determine the flux of the star.

In this paper, the aperture was chosen to have a radius of 10 pixels so as to be close to the FWHM, and the annulus was chosen to have an inner radius of 11 pixels and an outer radius of 16 pixels, sampling a small section of background sky just outside of the aperture.

2.7. *Photometry Table*

Once all of the magnitudes, magnitude errors, colors (like B-V for instance), and color errors have been calculated, an extra step must be taken to calibrate the photometry to match a standard photometric system. The exact observing conditions, including the telescope, detector, atmospheric interferences, etc., cannot be easily and accurately replicated, so the apparent magnitude of a star as measured by one observer may not be the same as measured by a different observer. Thus, we must calibrate our observed magnitude to match a standard system that will allow us to compare our derived measurements with other observers. This requires the use of a standard star that has a well known magnitude to help define the zero point, which acts as a calibration factor for our measured magnitudes.

In this paper, we select the standard star SA 20-245, having known magnitudes of 8.951, 8.475, and 9.817 in the V, R, and B bands, respectively. We use the following equation:

$$m_1 = -2.5log_{10}\mu_1 + 2.5log_{10}\mu_2 + m_2 \qquad (10)$$

where the first term is our instrumental magnitude, or the magnitude of a star in the cluster as measured by our telescope, and the sum of the second and third terms is the zero point, where m_2 is the magnitude of the standard star obtained from Landolt (2013) and $2.5log_{10}\mu_2$ is the magnitude of the standard star as calculated through the flux we measured. This equation can be rewritten in terms of the zero point (Z) as follows:

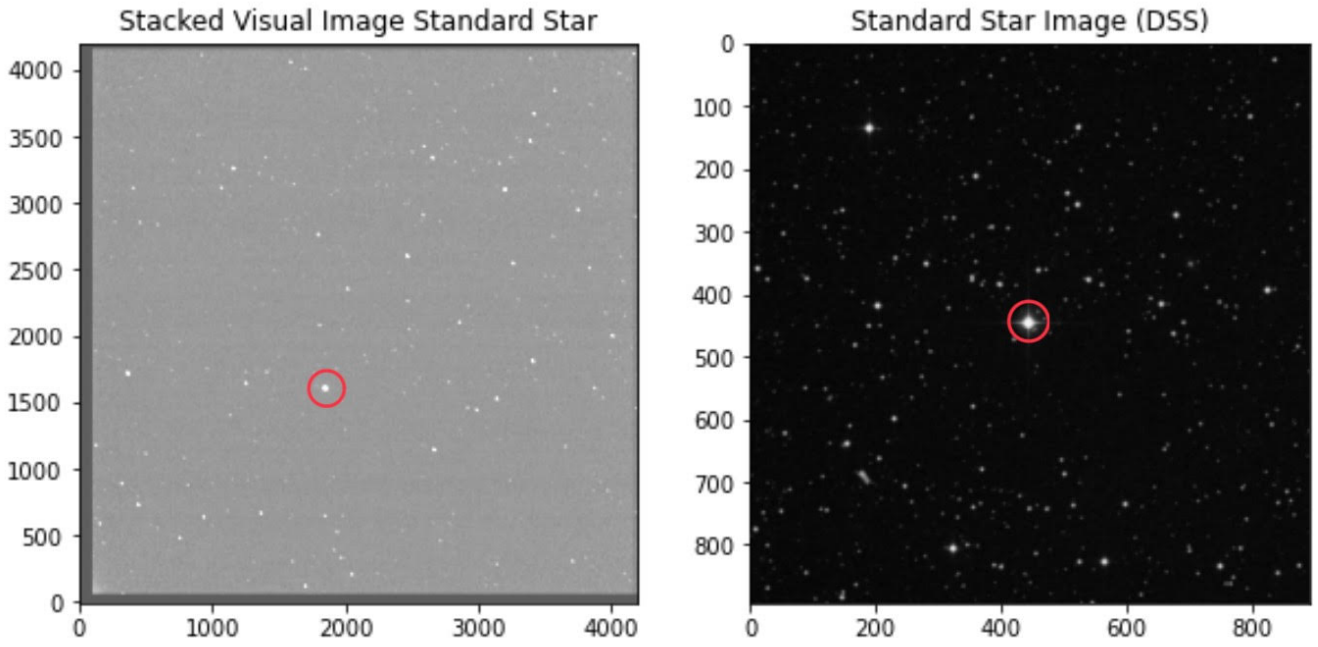

Figure 4. Comparison of the stacked visual image containing the standard star SA 20-245 vs the DSS image. The standard star can be seen circled in red.

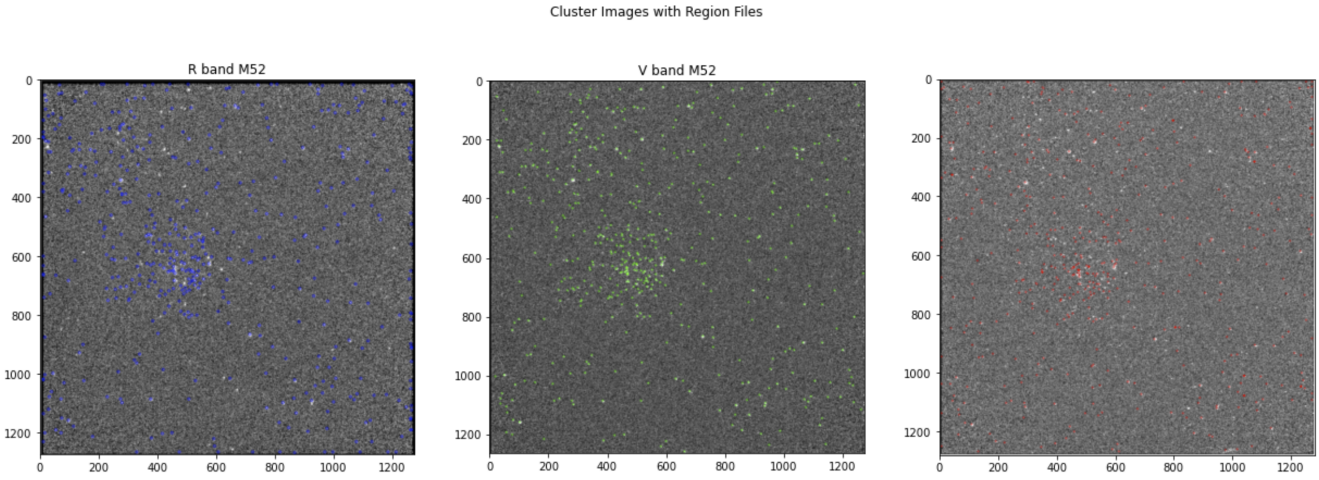

Figure 5. The region files, calculated using nsigma and the FWHM, in the three filter bands (blue, visual, and red) for the cluster M52.

$$m_1 = -2.5 log_{10}\mu_1 + Z \tag{11}$$

With these properly calibrated magnitudes of the stars in the cluster, in all three filter bands, we are then able to determine the B-V and V-R color indices by simply subtracting the magnitudes for each star. All of these quantities are appended to the photometry table for further use, as will be detailed in the next section.

3. RESULTS

3.1. *Color-Magnitude Diagram*

In this paper, we choose to make two CMDs, both of which plot the magnitude in the V band on the y-axis and then either B-V or V-R color on the x-axis, as our stacked images are in the B, V, and R bands. These quantities are obtained from the photometry table, where the columns are computed from the process detailed in Sections 2.6 and 2.7. We show the resulting CMD diagrams in Figure 7 and 8.

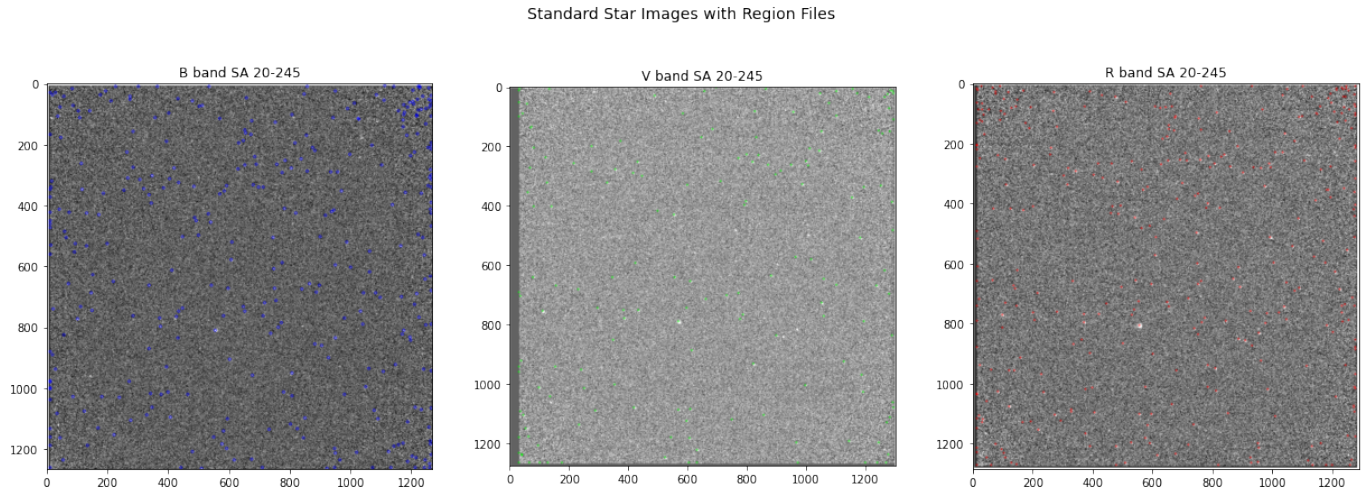

Figure 6. The region files, calculated using nsigma and the FWHM, in the three filter bands (blue, visual, and red) for the standard star.

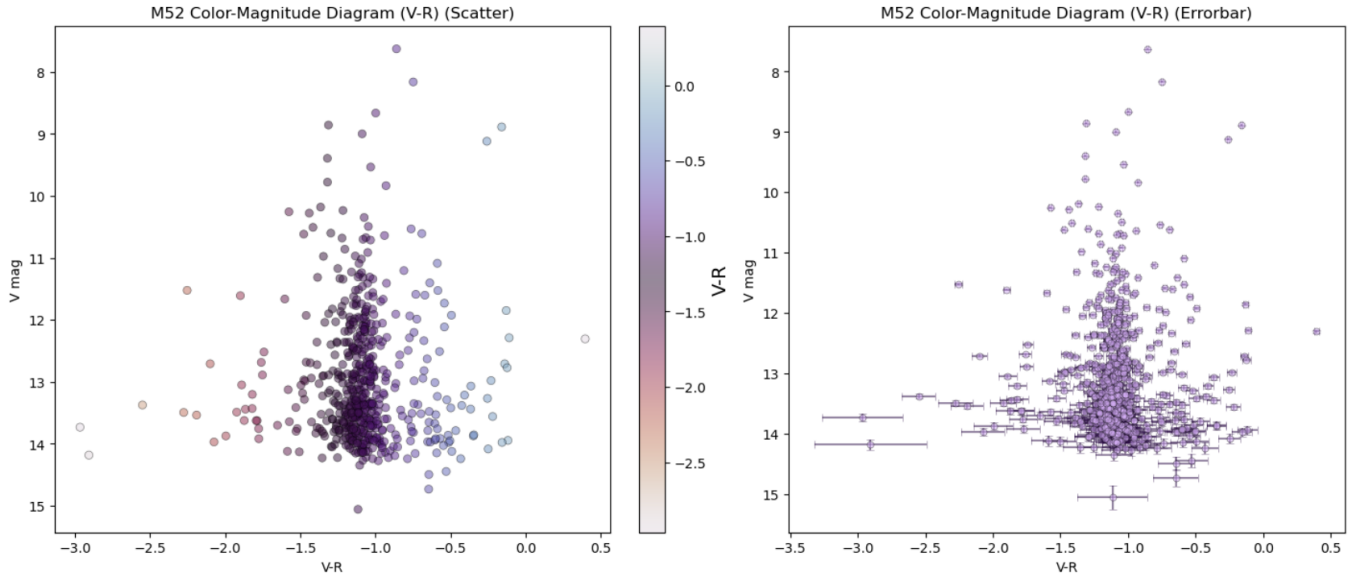

Figure 7. Color-magnitude diagram for the open cluster M52, showing the distribution of magnitude in the V-band vs V-R color and the errorbars.

3.2. *Isochrone Fitting*

In this paper, isochrone curves from P. Marigo1 & Granato2 (2008) were used to estimate the age of the cluster M52; the various isochrones can be seen in Figure 9, and the overplotted isochrones shifted to fit the data can be found in Figure 10. The curve correlating to a cluster age of 1e8 years was determined to have the best fit to the data plotted in the CMD as seen in Figure 9. This is similar to the literature value of the age of the cluster of 1.58e8 (Wu et al. 2009). The χ^2 value for this chosen isochrone is shown in Table 3.

Isochrone (age)	χ^2 (main sequence)
1e8	4054426.655

Table 3. The χ^2 value for the best isochrone age (1e8), compared along the main sequence. This value was not the lowest χ^2, but was one of the lowest, and had the best approximation for the upper distribution around the main sequence turn-off point and recently-forming red giant branch.

3.3. *Distance Modulus from Isochrone Fitting*

Isochrone fitting can also be compared to experimental data in order to calculate the distance modulus. The distance modulus is the distance to the cluster, which is determined by equation 4. In this paper, the distance

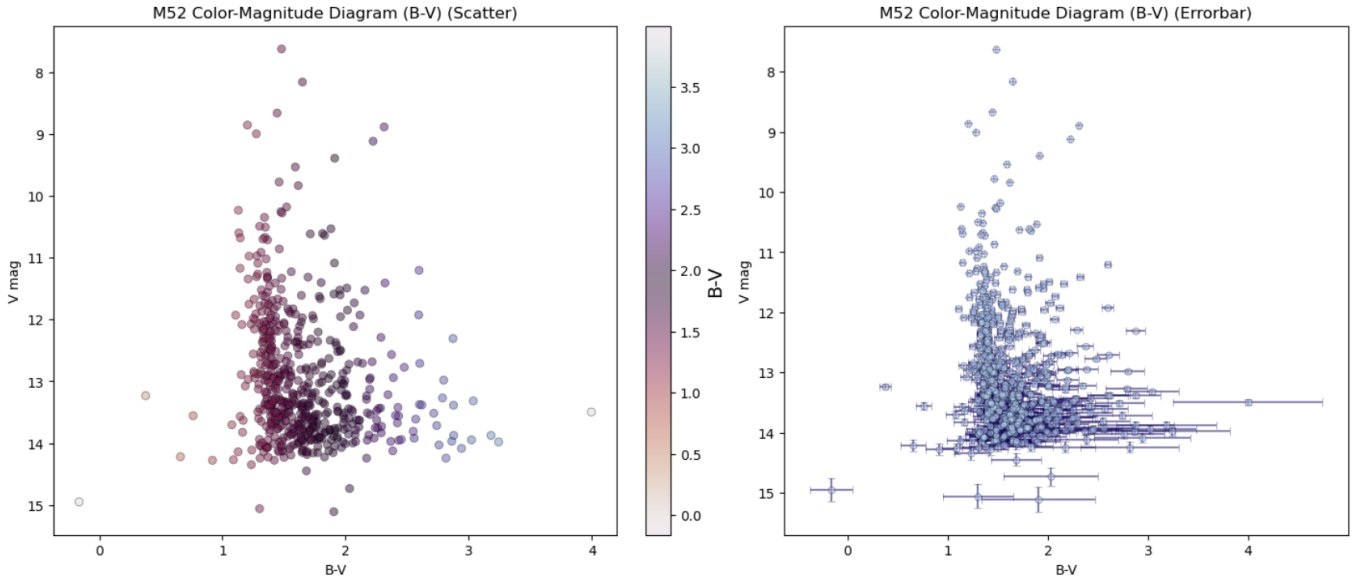

Figure 8. Color-magnitude diagram for the open cluster M52, showing the distribution of magnitude in the V-band vs B-V color and the errorbars.

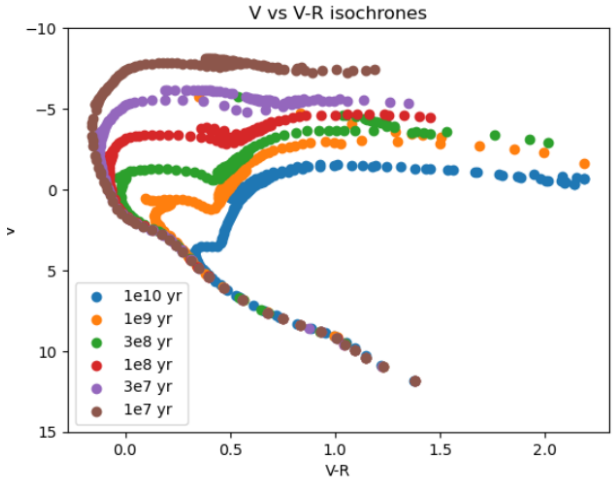

Figure 9. marigo08 Age Isochrones

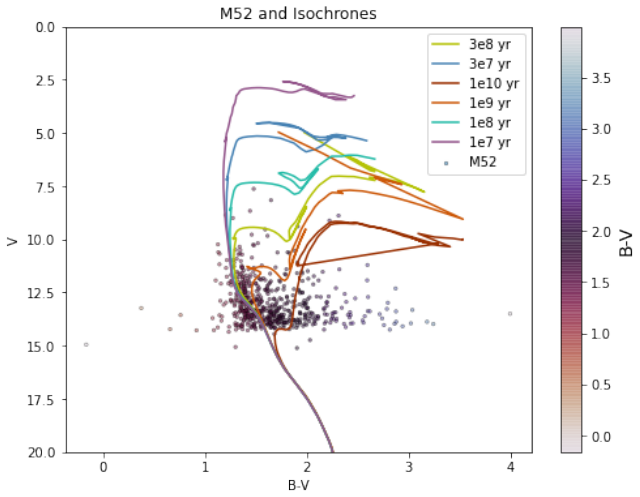

Figure 10. Color-magnitude diagram for the open cluster M52, showing the distribution of magnitude in the V-band vs B-V color, and the possible choices of isochrones.

modulus was calculated by taking the difference between the y-axis value between the isochrone plot and the experimental CMD plot at equivalent values on the x-axis. This difference in y-value is due to the difference in absolute magnitude (given by the isochrone) and apparent magnitude (given by the CMD data). We take this difference in magnitude to be the same value (10.7) that was used to shift the isochrone's V magnitude to better align with the M52 CMD data points. Using this, we conclude that the distance to the cluster is approximately 1380.38 parsecs, which is reasonable in comparison to the known distance of 1533 parsecs, yielding a -9.96% error.

3.4. *Sources of Error*

There are many potential sources of error in this research project. The biggest issue was the alignment of the final stacked B, V, and R images, as the shifting function did not seem to be working properly and consequently the images were becoming less aligned. We accounted for this issue by choosing the code that shifted the images the closest distance possible, and then manually aligning the images for the remaining distance. Within the shift function, there were occasional issues with padding the stacked images (adding a border on all four sides so that no detail is lost when shifting the images), as the padding showed as uneven widths at times despite being set to a fixed value. This issue seems

to have been resolved before aperture photometry took place. Ds9 (the software used to open astronomical issues) may have had some minor issues contributing as a source of error, for instance, if it did not correctly display the aligned images. Finally, the cluster, M52, is densely packed with stars towards its center, so there may have been issues where the aperture contained more than just the star of interest, which would have resulted in inaccurate flux values and likewise magnitudes. All of these issues could potentially contribute to the overall shape and distribution of the two CMDs shown in Section 3.1.

4. CONCLUSION

We conclude from the two CMDs that the open cluster M52 is a relatively young stellar population, which is supported by our choice of the cluster age 1e8 as the best-fit isochrone for our data. This matches expectations, as sources find the age of the cluster to fall within the range of 7th or 8th order of magnitude. With this age in mind, we would expect to see the main sequence (MS), with maybe only a few high mass stars turning off of the MS at this point in time, as their lifetimes are shorter than the remainder of the stellar population. The points at the top of the CMD, having the greatest luminosities and appearing more spread out on the diagram, are likely to be these bluer stars that are at the MS turnoff point. We can see many possible outliers in the higher and lower extremes of V-R and B-V color, which is likely responsible for the very vertical appearance of the CMD distribution. These outliers could have resulted from issues with the photometry table, of which the possible sources of error are detailed in Section 3.4. Alternatively, if the outliers are in fact the results of real data, their location on the plot suggests the presence of white dwarf stars and possibly low mass stars like brown dwarfs, though this is highly unlikely since white dwarfs form from stars having stellar masses less than that of our sun. This evolution to white dwarfs would therefore have not occurred yet since only the high mass bluer stars will be turning off the MS at this time. Further investigations would need to be conducted in order to determine the true source of these outliers, but the most likely explanation is that they are random artifacts that fit the criteria to be detected as stars, but are not truly stars.

In starting this project again from scratch, it would be helpful to have taken the flat frame images ourselves. Due to specific circumstances, we were unable to take those images and thus had to use data from another group, which is not ideal due to the possible differences in atmospheric and general conditions. Furthermore, it would be beneficial to do this project over a longer timescale, as many of the issues with alignment were difficult to resolve and the stacked images used in this paper had to be manually aligned to account for these issues (this is not a good practice in astronomy).

In the future, it would be interesting to perform similar research on open clusters of approximately the same age, and then compare their CMDs; this process may help to resolve both the cause of the outliers as well as the reason for why the CMD appears so vertical for this cluster). Moreover, it would be interesting to observe this cluster in different wavelength bands and plot a CMD of, for instance, I magnitude vs R-I color. Alternatively, we could image the cluster using a different telescope to compare the image resolution's impact on the derived photometry table and likewise the CMD. M52 is quite young and also very densely populated with stars; the possibilities of future studies are endless!

5. ACKNOWLEDGMENTS

This work was made possible through the use of Astropy and SAOImageDS9.

REFERENCES

Landolt, A. U. 2013, AJ, 146, 131,

doi: 10.1088/0004-6256/146/5/131

P. Marigo1, L. Girardi2, A. B. . M. A. T. G. L. S., & Granato2, G. L. 2008, Astronomy and Astrophysics, 482, 883, doi: https://doi.org/10.1051/0004-6361:20078467

Wu, Z.-Y., Zhou, X., Ma, J., & Du, C.-H. 2009, Monthly Notices of the Royal Astronomical Society, 399, 2146, doi: 10.1111/j.1365-2966.2009.15416.x

[b]